IEEE Access
Multidisciplinary ⋮ Rapid Review ⋮ Open Access Journal

Received 20 December 2022, accepted 13 January 2023, date of publication 19 January 2023, date of current version 24 January 2023.

*Digital Object Identifier 10.1109/ACCESS.2023.3238107*

RESEARCH ARTICLE

# Development and Analysis of a Detail Model for Steer-by-Wire Systems

**MARCUS IRMER[1,2], RENÉ DEGEN[1,2], ALEXANDER NÜßGEN[1,2], KARIN THOMAS[2], (Member, IEEE), HERMANN HENRICHFREISE[1], AND MARGOT RUSCHITZKA[1]**

[1]Faculty of Automotive Systems and Production, TH Köln—University of Applied Sciences, 50679 Cologne, Germany
[2]Ångströmlaboratoriet, Uppsala University, 75237 Uppsala, Sweden

Corresponding author: Marcus Irmer (marcus.irmer@th-koeln.de)

This work was supported by the Open Access Publication Fund of the TH Köln.

**ABSTRACT** Steer-by-wire systems represent a key technology for highly automated and autonomous driving. In this context, robust steering control is a fundamental precondition for automated vehicle lateral control. However, there is a need for improvement due to degrees of freedom, signal delays, and nonlinear characteristics of the plant which are unconsidered in the design models for the design of current steering controls. To be able to design an extremely robust steering control, suitable optimal models of a steer-by-wire system are required. Therefore, this paper presents an innovative nonlinear detail model of a steer-by-wire system. The detail model represents all characteristics of a real steer-by-wire system. In the context of a dominance analysis of the detail model, all dominant characteristics of a steer-by-wire system, including parameter dependencies, are identified. Through model reduction, a reduced model of the steer-by-wire system is then developed that can be used for a subsequent robust control design. Furthermore, this paper compares the steer-by-wire system with a conventional electromechanical power steering and shows similarities as well as differences.

**INDEX TERMS** Mechatronic systems, vehicle dynamic systems, steer-by-wire systems, modeling, model reduction.

## I. INTRODUCTION

Steer-by-wire (SbW) systems have become a key technology on the way to highly automated and autonomous driving and will therefore be used in modern vehicles. The advantages of SBW systems can for example be found in [1]. The difference between them and a conventional electromechanical power steering (EPS) system is that SbW systems no longer have a mechanical connection between the steering wheel and the front wheels (see Fig. 1). As a result, it is no longer possible to control the vehicle's lateral position if the steering control of the SbW system malfunctions. This could lead to a considerably dangerous situation. Thus, a guaranteed high robustness of the steering control in any driving situation is essential for SbW systems [1], [2]. However, current control approaches cannot guarantee this high robustness, as illustrated in [3], and often show only limited robustness to degrees of freedom and nonlinear characteristics of the plant which are neglected in the control design. To address this issue, this paper develops an innovative detail model of a SbW system that considers all relevant degrees of freedom and nonlinear characteristics that may occur in a real SbW system.

The associate editor coordinating the review of this manuscript and approving it for publication was Hassen Ouakad.

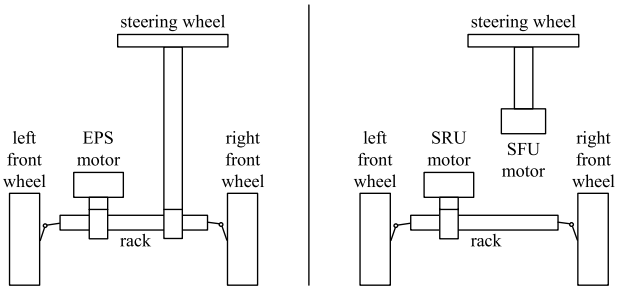


**FIGURE 1.** EPS system (left) and SbW system (right).

This detail model describes the real plant with a high degree of accuracy. It is introduced in chapter 2. The analysis of the detail model is then described in chapter 3. The model analysis is the basis for deriving corresponding optimal design models from the detail model, which is presented in chapter 4. In addition, chapter 5 compares the SbW system with a conventional EPS system and identifies similarities as well as differences. Finally, a summary is given in chapter 6.

## II. DETAIL MODEL OF THE STEER-BY-WIRE SYSTEM

In this chapter, an innovative nonlinear detail model of a SbW system is developed. The corresponding physical substitute model of the SbW system with nine degrees of freedom is shown in Fig. 2.

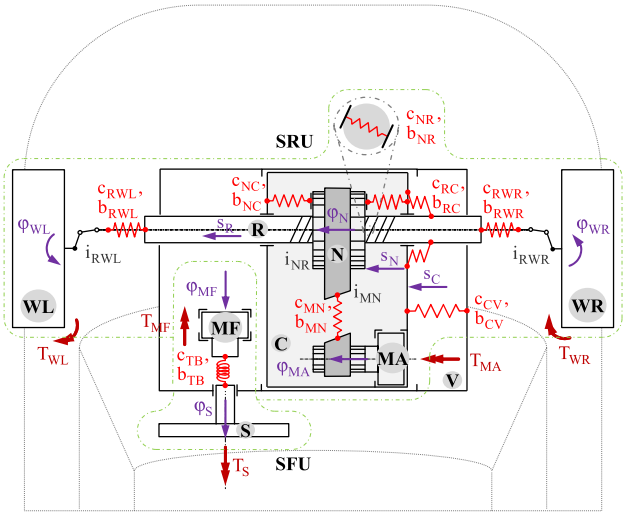


**FIGURE 2. Physical substitute model of the SbW system with nine degrees of freedom.**

The SbW system includes a steering wheel and a feedback actuator. Both are connected to each other via a torsion bar. Moreover, the SbW system contains a front axle actuator. It is connected via a belt drive to a nut, which in turn is connected via a ball screw drive to a rack and finally via the tie rods and levers to the left and right front wheel.

The resulting bodies of the multibody system are indicated in Fig. 2 by the labels S (steering), MF (feedback motor), MA (axle motor), N (nut), WL (wheel left), WR (wheel right), R (rack), C (casing), and V (vehicle). The degrees of freedom of the multibody system are illustrated with purple arrows in Fig. 2.

The nonlinear equations of motion of this physical substitute model are derived with the help of the Newton-Euler method [4], [5]. Starting point for this are the results of the kinematic analysis as well as the free-body system, which exposes the forces and torques acting on the individual bodies of the detail model. Based on this, the principle of linear and angular momentum for all bodies are formulated, which finally lead to the nonlinear equations of motion.

The detail SbW model is divided into a submodel for the steering feedback unit (SFU) and a submodel for the steering rack unit (SRU). Both units are mechanically decoupled (see Fig. 1 and Fig. 2). The SFU and the SRU are described in the following subsections.

### A. STEERING FEEDBACK UNIT

The steering feedback unit consists of the steering wheel and a current-controlled feedback actuator. The feedback actuator is also called SFU motor and is used to generate a desired steering feel for the driver. Both the steering wheel and the SFU motor are connected by a torsion bar [6]. The torsion bar is modeled by the stiffness $c_{TB}$ and the damping constant $b_{TB}$ (see Fig. 2). The steering wheel is modeled as a rotational mass with the moment of inertia $J_S$, the viscous friction $b_S$ and the angle $\varphi_S$. The mechanical part of the feedback motor including a corresponding gearing mechanism is modeled by a rotational mass transformed to steering wheel coordinates with the moment of inertia $J_{MF}$, the viscous friction $b_{MF}$ and the angle $\varphi_{MF}$.

By formulating the principle of angular momentum of the individual rotational masses, the differential equations

$$\begin{aligned} J_S\dot{\Omega}_S &= T_S - T_{TB} - b_S\Omega_S \\ J_{MF}\dot{\Omega}_{MF} &= -T_{MF} + T_{TB} - b_{MF}\Omega_{MF} \end{aligned} \tag{1}$$

for the mechanical part of the SFU model result. Here, $T_S$ describes the driver's steering torque, $T_{MF}$ describes the SFU motor torque transformed to steering wheel coordinates, acting in the opposite direction, and

$$T_{TB} = c_{TB}(\varphi_S - \varphi_{MF}) + b_{TB}(\Omega_S - \Omega_{MF}) \tag{2}$$

describes the torsion bar torque for $\varphi_S > \varphi_{MF}$ and $\Omega_S > \Omega_{MF}$. Hence, the mechanical part is modeled by a two-mass oscillator. Furthermore, the dynamic characteristics of the SFU motor control can be modeled by a first order lag system with the differential equation

$$\tau_{MF}\dot{T}_{MF} + T_{MF} = T_{MF_{rq}}, \tag{3}$$

as shown in [7]. Here, $\tau_{MF}$ is the time constant of the SFU motor control and $T_{MFrq}$ is the requested SRU motor torque. Equations (1) to (3) form the SFU model.

### B. STEERING RACK UNIT

The steering rack unit consists of the steering mechanism and a current-controlled front axle actuator. The front axle actuator is located in a so-called axis-parallel configuration parallel to the front axle resp. the rack, as shown in Fig. 2. Its task is to deflect the rack and thus the front wheels according to the steering wheel angle. The front axle actuator is also called SRU motor.

The mechanical part of the SRU model considers all relevant degrees of freedom and characteristics of a real steering mechanism. The corresponding bodies of the SRU are coupled by viscoelastic elements and gears. These are indicated by the labels $c_{xy}$ as well as $b_{xy}$ and $i_{xy}$ in Fig. 2. Here, the indices $x$ and $y$ specify between which two bodies the viscoelastic element or the gear is placed. The viscoelastic

elements and gears have partly nonlinear characteristics. The mechanical part of the SRU model has seven degrees of freedom (DOF). Therefore, the resulting overall SRU model is also called 7DOF model. The large number of degrees of freedom leads to a mathematical model with several coupled differential equations and additional ordinary equations. Due to the size, the equations are not illustrated here.

The dynamic characteristics of the SRU motor current control can be modeled analogously to chapter 2.1 by a first order lag system with the time constant $\tau_{MA}$ of the SRU motor control and the requested SRU motor torque $T_{MArq}$.

By coupling the model of the mechanical part with seven degrees of freedom and the model of the motor control, the detail SRU model is generated.

If this detail SRU model is combined with the SFU model from chapter 2.1, the detail SbW model results. The detail model for a SbW system presented here has nine degrees of freedom and outperforms the simple models from other publications as described in [3]. For this detail model, a comprehensive model analysis is demonstrated in the following section.

## III. MODEL ANALYSIS

In this chapter, the results of the analysis of the linearized detail SbW model are shown.

### A. STEERING FEEDBACK UNIT

Based on the approach of controlling the driver's steering torque [8], the SFU should provide the driver with a desired steering feel depending on the current driving situation [9], [10], [11], [12], [13]. The steering torque $T_S$ induced at the steering wheel corresponds to the steering feel experienced by the driver. At a constant steering angle $\varphi_S$, the steering torque $T_S$ is equal to the torsion bar torque $T_{TB}$. Since the steering torque $T_S$ cannot be measured, the torsion bar torque $T_{TB}$ is the controlled variable as a substitute for the steering torque $T_S$. The steering torque $T_S$ itself represents a disturbance variable for a corresponding control. The control variable is the requested SFU motor torque $T_{MFrq}$. Fig. 3 then shows the results of the model analysis of the control transfer path from the control variable $T_{MFrq}$ to the controlled variable $T_{TB}$ in form of the step response (top left), the pole-zero map (bottom left), as well as the frequency response (right).

In addition, Fig. 4 shows the results of the model analysis of the disturbance transfer path from the disturbance variable $T_S$ to the controlled variable $T_{TB}$, also in form of the step response (top left), the pole-zero map (bottom left), and the frequency response (right).

It can be seen that a conjugate complex eigenvalue pair dominates the dynamic behavior of the SFU. The eigen-frequency at about 150 rad/s (24 Hz) of the corresponding oscillation can be described by the equation

$$\omega_0 = \sqrt{\frac{c_{TB}}{J_{res}}} \tag{4}$$

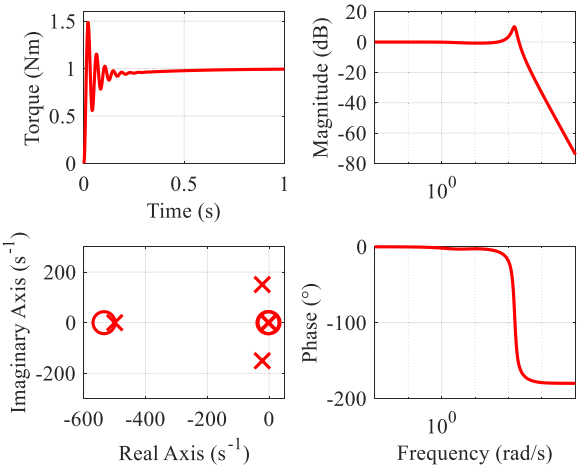


**FIGURE 3.** Step response (top left), pole-zero map (bottom left), and frequency response (right) of the control transfer path of the SFU model from the requested SFU motor torque $T_{MFrq}$ to the torsion bar torque $T_{TB}$.

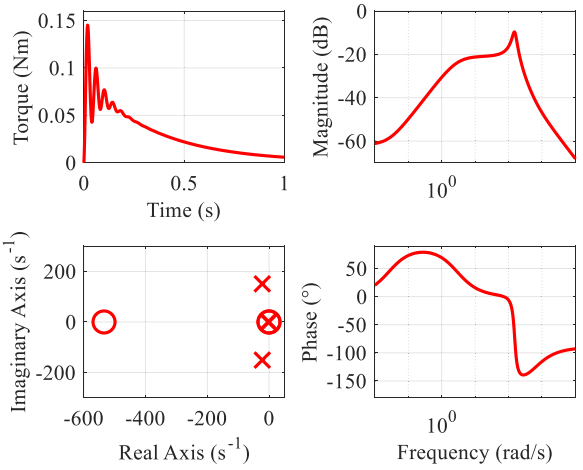


**FIGURE 4.** Step response (top left), pole-zero map (bottom left), and frequency response (right) of the disturbance transfer path of the SFU model from the steering torque $T_S$ to the torsion bar torque $T_{TB}$.

with

$$J_{res} = \frac{J_S J_{MF}}{J_S + J_{MF}}. \tag{5}$$

It thus depends on the stiffness $c_{TB}$ of the torsion bar as well as on the moments of inertia $J_S$ and $J_{MF}$ of the steering wheel and the SFU motor.

### B. STEERING RACK UNIT

The SRU should convert a driver's steering request into a corresponding deflection $s_R$ of the rack. The deflection $s_R$ is therefore the controlled variable and the requested SRU motor torque $T_{MArq}$ is the control variable. Disturbance variables are the torques $T_{WL}$ and $T_{WR}$ about the steering axes of the left and right front wheel. These torques correspond to the tire forces and torques according to the current driving situation. Fig. 5 then shows the results of the model analysis of the control transfer path from the control variable $T_{MArq}$ to the controlled variable $s_R$ in form of the step response (top left),

the pole-zero map (bottom left), and the frequency response (right). For better visualization, the two high-frequency zeros of this transfer path at about -58 000 and -61 000 are not shown.

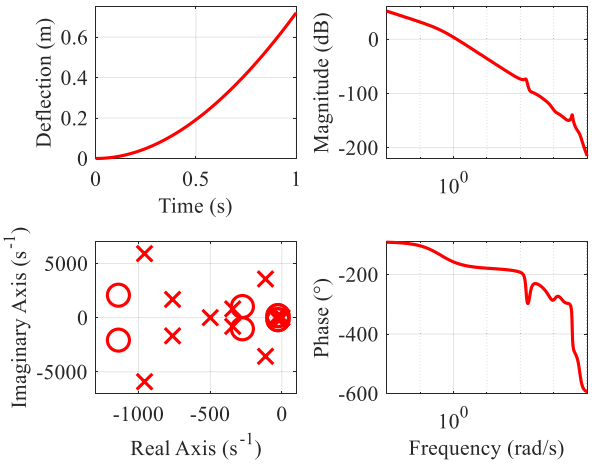


**FIGURE 5.** Step response (top left), pole-zero map (bottom left), and frequency response (right) of the control transfer path of the SRU model from the requested SRU motor torque $T_{MArq}$ to the deflection $s_R$ of the rack.

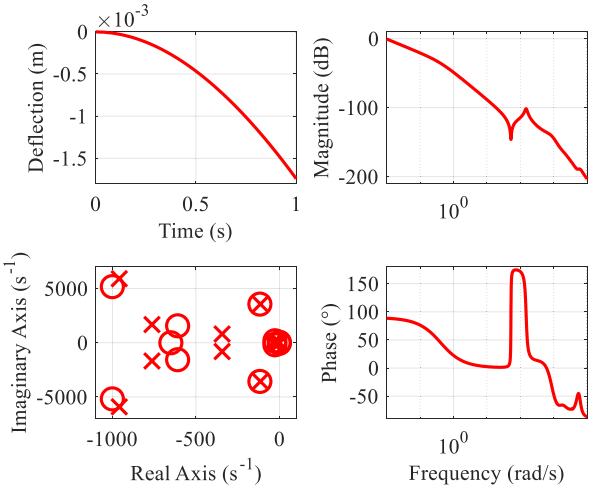


**FIGURE 6.** Step response (top left), pole-zero map (bottom left), and frequency response (right) of the disturbance transfer path of the SRU model from the disturbance torque $T_{WL}$ at the left front wheel to the deflection $s_R$ of the rack.

In addition, Fig. 6 shows the results of the model analysis of the disturbance transfer path from the disturbance variable $T_{WL}$ to the controlled variable $s_R$, also in form of the step response (top left), the pole-zero map (bottom left), and the frequency response (right).

Due to the symmetry of the steering mechanism, the results of the model analysis of the second disturbance transfer path of the SRU model from the disturbance torque $T_{WR}$ to the controlled variable $s_R$ look identical to Fig. 6. The corresponding results are therefore not illustrated here. The two disturbance torques $T_{WL}$ and $T_{WR}$ are consequently often combined in other publications to generate only one disturbance variable in the form of a disturbance force at the rack.

The dynamic behavior of the SRU is characterized by several conjugate complex eigenvalue pairs. To highlight the positions of the corresponding eigenfrequencies (black circled digits), the frequency response of the control transfer path of the damped and undamped SRU model is shown in Fig. 7. In addition, the notch frequencies (gray circled digits) of the control transfer path are also visible there.

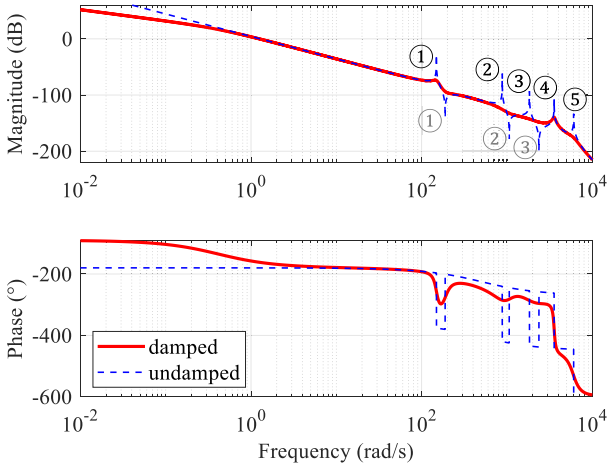


**FIGURE 7.** Frequency response of the control transfer path of the damped and undamped SRU model from the requested SRU motor torque $T_{MArq}$ to the deflection $s_R$ of the rack.

The frequency response can be used to show the influence of a variation of individual parameters on the characteristics of the SRU. For example, the first eigenfrequency at about 150 rad/s (24 Hz) corresponding to the most dominant eigenvalue pair can be determined very well by the equation

$$\omega_0 \approx \sqrt{\frac{c_{res}}{J_{res}}} \tag{6}$$

with

$$c_{res} = \frac{c_{RW} c_{MR}}{c_{RW} + c_{MR}}, \tag{7}$$

$$c_{MR} = \frac{c_{NR} c_{NC} c_{CV}}{c_{NR} c_{NC} + c_{NR} c_{CV} + c_{NC} c_{CV}}, \tag{8}$$

and

$$J_{res} = \frac{\frac{J_W}{i_{RW}^2}(J_{MA} + \frac{J_N}{i_{MN}^2}) i_{MN}^2 i_{NR}^2}{\frac{J_W}{i_{RW}^2} + (J_{MA} + \frac{J_N}{i_{MN}^2}) i_{MN}^2 i_{NR}^2}. \tag{9}$$

Here, $i_{RW}$ describes the average gear ratio and $c_{RW}$ as well as $J_W$ the total stiffness and the total moment of inertia of the left and right wheel attachment. Furthermore, the first notch frequency at about 190 rad/s (30 Hz) can be approximated by the equation

$$\omega_T \approx \sqrt{\frac{c_{RW}}{\frac{J_W}{i_{RW}^2}}}. \tag{10}$$

The location of the lowest eigen- and notch frequencies thus depends mainly on the parameters of the front wheels and

the wheel attachments. A stiffer connection $c_{RW}$ of the front wheels to the rack increases the eigen- and notch frequencies. A larger wheel inertia $J_W$, on the other hand, reduces them. A change in the gear ratio $i_{RW}$ between the rack and front wheel also primarily affects only these eigen- and notch frequencies.

In addition, the stiffnesses $c_{NC}$, $c_{CV}$, $c_{NR}$, and $c_{MN}$ of the axial nut bearing, the casing attachment, the ball screw drive, and the belt drive between the SRU motor and the nut have only a significant influence on the location of the high-frequency eigen- and notch frequencies. Here, the eigen- and notch frequencies increase with increasing stiffness and vice versa. This insight can be used in the following model reduction.

By analyzing the corresponding nonlinear model, the conclusions drawn here can be reconfirmed. Hence, the results are not shown.

## IV. MODEL REDUCTION

For a subsequent controller and observer design, a SbW model of the lowest possible order is required. Therefore, in this chapter a reduced SbW model is derived from the detail SbW model. This reduced model replicates all the dominant characteristics of a real SbW system.

### A. STEERING FEEDBACK UNIT

The mechanical part of the SFU model has two degrees of freedom and corresponds to a two-mass oscillator. Hence, it already represents a model of low order and does not have to be reduced further.

### B. STEERING RACK UNIT

The mechanical part of the SRU model has seven degrees of freedom and thus a correspondingly high order. In addition, it has high-frequency characteristics that are for example not suitable for real-time simulation. Therefore, it needs to be reduced.

If all the connections between the bodies of the SRU are assumed to be rigid, the model of the mechanical part with seven degrees of freedom is transformed into a reduced model of the mechanical part of the SRU with only one degree of freedom. Such a simple model like in [14], [15], [16], and [17] is currently often used for the design of controls for SbW systems. However, a control system created with such a design model does not show good robustness characteristics against unconsidered eigenmodes [3].

Since the viscoelastic wheel attachments usually have a much lower stiffness than the remaining viscoelastic elements of the SRU ($c_{RW} \ll c_{MR}$), the dominant behavior of the SRU is thus determined by the parameters of the viscoelastic wheel attachments according to (6) to (10). Therefore, a better model of the SRU with two degrees of freedom can be developed based on the results of the model analysis from chapter 3.2 by a physically motivated order reduction which reproduces this dominant characteristic of a real SRU. Consequently, the reduced model corresponds to a two-mass oscillator with one degree of freedom for the SRU motor angle $\varphi_{MA}$ and one degree of freedom for a substitute angle $\varphi_W$ of the front wheels. It is derived from the detail SRU model with seven degrees of freedom by introducing constraints for the assumptions that the belt drive between SRU motor and nut is rigid and that the front wheels always deflect with the same angle. In addition, small masses and inertias are redistributed to the remaining bodies and the resulting model is statically condensed. Then, the substitute stiffness of the statically condensed model can be approximated using (7) and (8).

The SRU model consisting of this reduced model of the mechanical part of the SRU with two degrees of freedom and the current-controlled SRU motor is called 2DOF model in the subsequent sections.

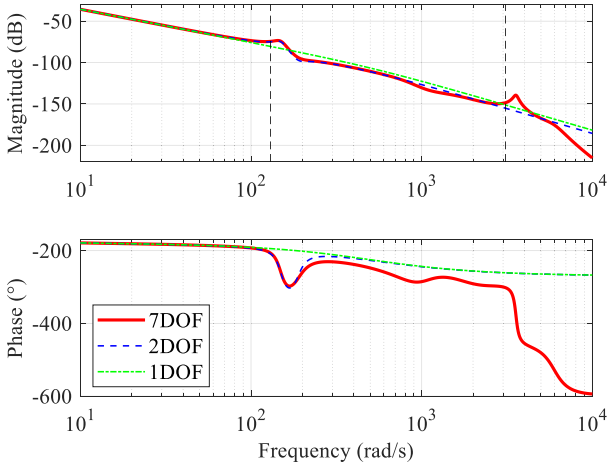


**FIGURE 8. Frequency response of the control transfer path of the 7DOF, 2DOF, and 1DOF model of the SRU from the requested SRU motor torque $T_{MArq}$ to the deflection $s_R$ of the rack.**

Fig. 8 shows the frequency response of the control transfer path of the 7DOF model as well as the 2DOF model of the SRU. In addition, the frequency response of a 1DOF model of the SRU, as currently often used for the design of steering controls, is also displayed.

It can be seen that the developed 2DOF model maps the 7DOF model with sufficient accuracy up to frequencies of 3100 rad/s (490 Hz), whereas the frequency response of the 1DOF model already differs significantly from the frequency response of the 7DOF model at frequencies of 130 rad/s (20 Hz). Consequently, the 1DOF model is not suitable for a control design, since the corresponding control would have only a small bandwidth and no high robustness.

The good conformity of the reduced 2DOF model with the detailed 7DOF model can also be seen by examining the eigenmodes of the models. Especially the eigenmodes corresponding to the lowest eigenfrequencies are relevant, since the other eigenfrequencies are beyond the supposed bandwidth of a possible control. Therefore, Fig. 9 shows the eigenmodes for the first eigenfrequency of the detailed 7DOF model of the SRU. The eigenmodes for the first (and only) eigenfrequency of the reduced 2DOF model of the SRU are

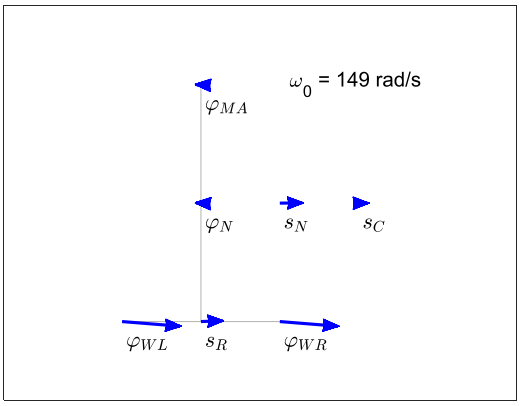


**FIGURE 9.** Eigenmodes for the first eigenfrequency of the 7DOF model of the SRU.

shown in Fig. 10. There, the amplitudes are normalized to a common level. With the previously introduced assumption that the front wheels can only deflect in the same direction, the corresponding amplitudes and phase angles of the left and right front wheel are identical ($\varphi_W = \varphi_{WL} = \varphi_{WR}$). Nevertheless, the amplitudes and phase angles of both front wheels are shown in the eigenmodes for a better comparison with the 7DOF model.

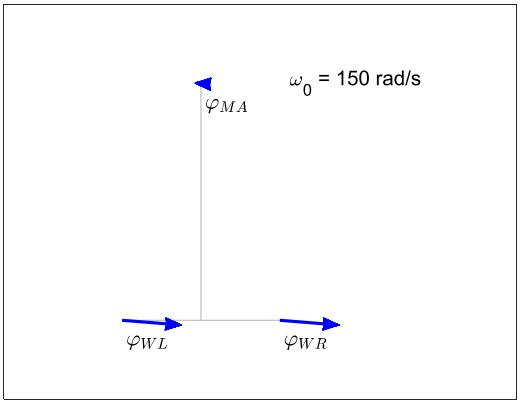


**FIGURE 10.** Eigenmodes for the first eigenfrequency of the 2DOF model of the SRU.

The comparison of the eigenmodes shows that the reduced 2DOF model and the detailed 7DOF model have a highly similar behavior in the low-frequency range, where the deflections of the wheels are dominant. From the plot for the 7DOF model in Fig. 9, it can also be seen that the elastic connections with the associated stiffnesses $c_{NR}$, $c_{NC}$, and $c_{CV}$ for the ball screw drive, the axial nut bearing, and the casing attachment experience a deformation, since the amplitudes and phase angles are different for the degrees of freedom $s_R$, $\varphi_N$, $s_N$, and $s_C$. Thus, these stiffnesses affect this eigenmodes. In contrast, the elastic connection between the SRU motor and the nut with the stiffness $c_{MN}$ of the belt drive hardly experiences any deflection, since the amplitudes and phase angle for the degrees of freedom $\varphi_{MA}$ and $\varphi_N$ are almost identical. Consequently, this elastic connection can be neglected, as it was also the case for the model reduction. So, based on the eigenmodes, the previously made assumptions for the model reduction can be confirmed once again.

The combination of the reduced 2DOF model of the SRU and the SFU model yields the optimal reduced SbW model, which can be used for a subsequent design of a highly robust steering control system.

An advantage of the developed method for the order reduction is that, if required, reduced models of most different order can be generated in a simple way, which show an optimal behavior for their respective application.

## V. MODEL COMPARISON

In this chapter, the identified characteristic behavior of a SbW system is compared with the characteristic behavior of an EPS system, which is currently mainly equipped in motor vehicles [18]. For this purpose, a detail model of an EPS system is used that was developed analogously to the method described in chapter 2. This model is for example illustrated in [3]. For a better comparability, the parameterization of the detail EPS model was selected to be the same as the parameterization of the detail SbW model.

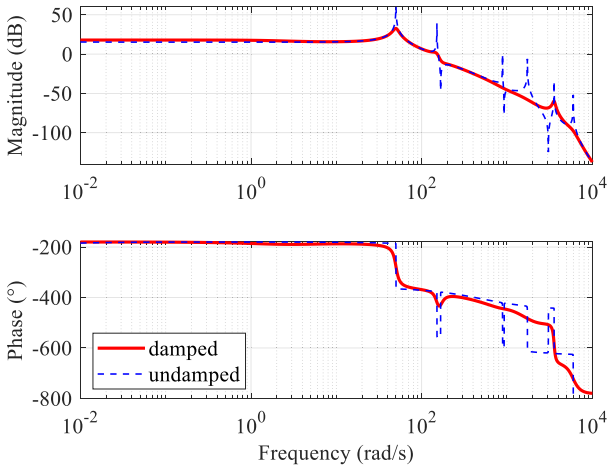


**FIGURE 11.** Frequency response of the control transfer path of the damped and undamped EPS model from the requested motor torque $T_{Mrq}$ to the torsion bar torque $T_{TB}$.

Fig. 11 then shows the frequency response of the control transfer path of the damped and undamped EPS model. Like the SFU model (see chapter 3.1), the eigenmodes for the lowest eigenfrequency at about 50 rad/s (8 Hz) are affected by the torsion bar in the steering column. The corresponding eigenfrequency can be approximated by (4), where the resulting moment of inertia $J_{res}$ is now composed of the moments of inertia of all bodies of the EPS model according to equation

$$J_{res} = \frac{J_S J_{down}}{J_S + J_{down}} \tag{11}$$

with

$$J_{down} = J_P + \frac{J_N i_{NR}^2}{i_{PR}^2} + \frac{J_M i_{MN}^2 i_{NR}^2}{i_{PR}^2} + \frac{m_R}{i_{PR}^2} + \frac{J_W}{i_{PR}^2 i_{RW}^2} \tag{12}$$

due to the mechanical connection between the steering wheel and the rack. Here, $J_P$ describes the moment of inertia of the pinion at the lower end of the steering column and $i_{PR}$ the gear ratio between the pinion and the rack. In addition, $J_{down}$ represents the substitute moment of inertia of all the bodies of the downstream of the EPS system. Since it is generally true that $J_{MF} \ll J_{down}$, the resulting moment of inertia $J_{res}$ of an EPS system according to (11) and (12) is significantly larger than the resulting moment of inertia of the SFU of a SbW system according to (5). So, the lowest eigenfrequency of the EPS model at about 50 rad/s (8 Hz) is lower compared to the lowest eigenfrequency of the SFU model of about 150 rad/s (24 Hz). In addition, the corresponding oscillation of the EPS model has a lower damping factor d than the oscillation of the SFU model according to equation

$$d = \frac{\omega_0 b_{TB}}{2c_{TB}} \tag{13}$$

because of its lower eigenfrequency.

The eigenmodes for the second lowest eigenfrequency at about 150 rad/s (24 Hz) correspond with sufficient accuracy to the eigenmodes for the lowest eigenfrequency of the SRU model (see chapter 3.2). This is the case because the resulting moment of inertia $J_{res}$ of the EPS model is dominated by the substitute moment of inertia $J_{down}$ of the downstream according to (11) and (12) with $J_S \ll J_{down}$. Normalized to a common level, this substitute moment of inertia is approximately equal to the resulting moment of inertia of the SRU model. The same is true for the eigenmodes corresponding to the high-frequency eigenfrequencies.

A comprehensive analysis of the detail EPS model can be found in [19], [20], [21], [22], and [23].

## VI. CONCLUSION AND OUTLOOK

This paper describes the modeling and analysis of a detail model for a steer-by-wire system (SbW system) consisting of a model of the steering rack unit (SRU) and a model of the steering feedback unit (SFU). The detail model represents all the characteristics of a real SbW system.

The detail model was subjected to a comprehensive analysis. Both the parameter dependencies and the dominant characteristics of the SbW system were identified. For example, it was shown that the dynamic behavior of the SRU is dominated by the viscoelastic wheel attachments. Therefore, both the SRU and the SFU can be modeled by a two-mass oscillator. Consequently, the reduced SbW model consists of the combination of these two two-mass oscillators. By means of a physically motivated order reduction, the parameters of the reduced model were optimized in such a way that the behavior of the reduced SbW model is congruent with the behavior of the detail SbW model up to excitation frequencies of more than 3100 rad/s (490 Hz).

In the next step, a control design for the control of the driver's steering torque and the rack deflection is performed based on the optimized reduced SbW model. Afterwards, the reference value specifications can be designed. This is the subject of further work.

## REFERENCES


[1] S. A. Mortazavizadeh, A. Ghaderi, M. Ebrahimi, and M. Hajian, "Recent developments in the vehicle steer-by-wire system," *IEEE Trans. Transport. Electrific.*, vol. 6, no. 3, pp. 1226–1235, Sep. 2020, doi: 10.1109/TTE.2020.3004694.

[2] R. Isermann, R. Schwarz, and S. Stolzl, "Fault-tolerant drive-by-wire systems," *IEEE Control Syst.*, vol. 22, no. 5, pp. 64–81, Oct. 2002, doi: 10.1109/MCS.2002.1035218.

[3] M. Irmer and H. Henrichfreise, "Design of a robust LQG compensator for an electric power steering," in *Proc. 21st IFAC World Congr.*, Jul. 2020, pp. 6624–6630, doi: 10.1016/j.ifacol.2020.12.082.

[4] W. Schiehlen and P. Eberhard, *Applied Dynamics*. Cham, Switzerland: Springer, 2014, doi: 10.1007/978-3-319-07335-4.

[5] F. Pfeiffer, *Mechanical System Dynamics*. Berlin, Germany: Springer, 2008, doi: 10.1007/978-3-540-79436-3.

[6] R. Gonschorek and T. Bertram, "Linear-quadratic-Gaussian position control of the hand wheel actuator for a steer-by-wire steering system," *Proc. Digit.-Fachtagung Mechatronik*, vol. 2021, pp. 110–115, Mar. 2021.

[7] E. Farshizadeh, "Regelungskonzept für eine elektrohydraulische Bremsanlage mit adaptivem Bremsgefühl," Ph.D. dissertation, Fac. Mech. Eng., Otto-von-Guericke-Universität Magdeburg, Magdeburg, Germany, 2017.

[8] H. Henrichfreise, J. Jusseit, and H. Niessen, "Optimale Regelung einer elektromechanischen Servolenkung," *Proc. Fachtagung Mechatronik*, vol. 2003, pp. 381–400, May 2003.

[9] M. Irmer and H. Henrichfreise, "Robust generation of a steering feel for electric power steering systems," *Proc. Digit.-Fachtagung Mechatronik*, vol. 2021, pp. 116–121, Mar. 2021.

[10] D. Cheon, C. Lee, S. Oh, and K. Nam, "Description of steering feel in Steer-by-Wire system using series elastic actuator," in *Proc. IEEE Vehicle Power Propuls. Conf. (VPPC)*, Oct. 2019, pp. 1–4, doi: 10.1109/VPPC46532.2019.8952490.

[11] S. Grüner, T. Werner, and B. Käpernick, "Objectification of steering feel and application in the context of virtual steering feel tuning," in *Proc. 8th Int. Munich Chassis Symp.*, Jun. 2017, pp. 289–306, doi: 10.1007/978-3-658-18459-9_20.

[12] A. Balachandran and J. C. Gerdes, "Designing steering feel for steer-by-wire vehicles using objective measures," *IEEE/ASME Trans. Mechatronics*, vol. 20, no. 1, pp. 373–383, Feb. 2015, doi: 10.1109/TMECH.2014.2324593.

[13] O. Graßmann, H. Henrichfreise, H. Niessen, and K. V. Hammel, "Variable Lenkunterstützung für eine elektromechanische Servolenkung," in *Proc. 23rd Tagung Elektronik Kraftfahrzeug*, Jun. 2003, pp. 78–84.

[14] A. H. El-Shaer, S. Sugita, and M. Tomizuka, "Robust fixed-structure controller design of electric power steering systems," in *Proc. Amer. Control Conf.*, Jun. 2009, pp. 445–450, doi: 10.1109/ACC.2009.5160219.

[15] S. M. H. Fahami, H. Zamzuri, S. A. Mazlan, and M. A. Zakaria, "Modeling and simulation of vehicle steer by wire system," in *Proc. IEEE Symp. Humanities, Sci. Eng. Res.*, Jun. 2012, pp. 765–770, doi: 10.1109/SHUSER.2012.6268992.

[16] M. Bertoluzzo, G. Buja, R. Menis, and G. Sulligoi, "An approach to steer-by-wire system design," in *Proc. IEEE Int. Conf. Ind. Technol.*, Dec. 2005, pp. 443–447, doi: 10.1109/ICIT.2005.1600679.

[17] A. Badawy, J. Zuraski, F. Bolourchi, and A. Chandy, "Modeling and analysis of an electric power steering system," in *Proc. Steering Suspension Technol. Symp.*, Mar. 1999, pp. 1–9, doi: 10.4271/1999-01-0399.

[18] P. Pfeffer and M. Harrer, *Lenkungshandbuch—Lenksysteme, Lenkgefühl, Fahrdynamik von Kraftfahrzeugen*, 2nd ed. Berlin, Germany: Springer, 2013, doi: 10.1007/978-3-658-00977-9.

[19] M. Irmer and H. Henrichfreise, "Design of a simulation environment for testing the control of electric power steering systems," in *Proc. 21st Internationales Stuttgarter Symp.*, Mar. 2021, pp. 521–533, doi: 10.1007/978-3-658-33521-2_35.

[20] M. Hemmersbach, H. Briese, M. Haßenberg, M. Irmer, and H. Henrichfreise, "Application of a detailed model of a steering system in highly dynamic HiL tests of EPS motors," in *Proc. 21. Internationales Stuttgarter Symp.*, Mar. 2021, pp. 534–545, doi: 10.1007/978-3-658-33521-2_36.
[21] M. Irmer, M. Haßenberg, H. Briese, and H. Henrichfreise, "Mechatronic system design for EPS systems with residual modes and variable, nonlinear plant behavior," in *Proc. 20th Internationales Stuttgarter Symp.*, Mar. 2020, pp. 469–482, doi: 10.1007/978-3-658-29943-9_36.
[22] M. Irmer, M. Haßenberg, H. Briese, and H. Henrichfreise, "Robust control of an electric power steering with unconsidered modes and parameter uncertainties," in *Proc. 10th Int. Munich Chassis Symp.*, vol. 2019, Jun. 2019, pp. 465–479, doi: 10.1007/978-3-658-26435-2_32.
[23] G. Wittler, M. Haßenberg, H. Briese, T. Schubert, and H. Henrichfreise, "Systematic model-based vibration analysis of a controlled electric power steering system," in *Proc. 8th Int. Munich Chassis Symp.*, vol. 2017, Jun. 2017, pp. 505–517, doi: 10.1007/978-3-658-18459-9_34.

**MARCUS IRMER** received the B.Eng. degree in mechatronics from the Hamm-Lippstadt University of Applied Sciences, Germany, in 2017, and the M.Sc. degree in mechatronics from the TH Köln—University of Applied Sciences, Germany, in 2019. He is currently pursuing the joint Ph.D. degree in cooperation with Uppsala University, Sweden, and TH Köln.

Since 2019, he has been a Research Associate with the Cologne Laboratory of Mechatronics and the CAD CAM Center Cologne, TH Köln. His research interest includes the area of model-based mechatronic system development. In this context, he focuses on the development and validation of innovative control strategies for steering systems.

**RENÉ DEGEN** received the M.Sc. degree in mechatronics from the TH Köln—University of Applied Science, Germany, in 2018. He is currently pursuing the joint Ph.D. degree in cooperation with Uppsala University, Sweden, and TH Köln.

From 2017 to 2020, he has been a Research Associate with the CAD CAM Center Cologne, TH Köln. In 2020, he became a Chief Engineer at the CAD CAM Center Cologne for the field of mechatronics. He focuses on the development of a virtual test environment for highly automated vehicle systems. His research interests include the field of robotics, mechatronics, and future mobility systems.

**ALEXANDER NÜßGEN** received the M.Sc. degree in automotive engineering from the TH Köln—University of Applied Sciences, Germany, in 2020. He is currently pursuing the Ph.D. degree in cooperation with Uppsala University, Sweden, and TH Köln.

Since 2018, he has been a Research Associate with the CAD CAM Center Cologne, TH Köln, with a particular focus on mathematical optimization questions using artificial intelligence. In 2021, he became a Chief Engineer at the CAD CAM Center Cologne for the field of mathematics. His main topics of data intelligence and strategic knowledge assessment within the mechatronic product development.

**KARIN THOMAS** (Member, IEEE) received the master's degree in engineering physics and the Ph.D. degree in engineering physics with specialization in electricity from Uppsala University, Sweden, in 2003 and 2008, respectively.

She was appointed Docent in engineering science with specialization in electricity, in 2020. She is currently employed as an Associate Professor at the Department of Electrical Engineering, Uppsala University, and as a Visiting Professor at Mälardalen University, Sweden. Previously, she has been working as an Assistant Professor and as a Development Engineer at Wave Power Company. She is also involved in research related to power system stability, grid connection of distributed renewable electricity generation, and charging of electric vehicles.

**HERMANN HENRICHFREISE** received the Dr. Ing. degree and the Diploma degree in mechanical engineering and the Ph.D. degree from Paderborn University, Germany, in 1983 and 1988, respectively.

In 1987, he was the Co-Founder of dSPACE Company. From 1987 to 1994, he was moreover a Chief Execute Officer of dSPACE Company. Since 1993, he has been a Professor in mechatronics with the TH Köln—University of Applied Sciences, Germany, where he established the Cologne Mechatronics Laboratory, in 1996. In 2001, he was the Co-Founder of DMecS Company. His research interests include theoretical principles, tools, and methods of mechatronics and their practical application.

**MARGOT RUSCHITZKA** received the Dr. rer. nat degree and the Diploma degree in mathematics from RWTH Aachen University, Germany.

She worked as a Research Associate at the Laboratory for Machine Tools (WZL), RWTH Aachen University. She continued her professional career as a Calculation Engineer at Company ABAQUS, Aachen, Germany. She took the position of the authorized signatory in the "Zentrum für Industrielle Anwendungen Massiver Parallelität" in Herzogenrath, Germany. Later on, she changed to self-employment as management consultant for innovation and technology. Since 1997, she has been a Professor in engineering mathematics and data processing at the TH Köln—University of Applied Sciences, Germany. As the Head of the CAD CAM Center Cologne and the Master Program Mechatronics at the Faculty of Vehicle Systems and Production her teaching and research activities focus on the area of optimization of innovation processes and virtual product development.